

## CHAPTER 211

### On Residual Transport in Shallow Tidal Basins <sup>1</sup>

Andrea Balzano <sup>2</sup>

#### Abstract

In the paper the influence of some physical and numerical effects on computations of residual transport in shallow tidal basins is analysed. Investigations deal with: i) the Coriolis acceleration, ii) the specification of the tidal forcing, iii) the diffusion coefficient, iv) a time weight in a standard implicit numerical scheme. The analysis has been carried out by means of intratidal mathematical models with reference to three schematic basins, with the tide being the only forcing of the system. These are typical conditions in which critical environmental events like anoxia occur. Usual assumptions in mathematical modeling of 2D flows in shallow basins regarding the above effects are tested both in the short and long term. The different importance of that effects depending on both the time scale of processes and the basin morphology is shown. Results are presented in terms of turbulence-time-averaged circulation patterns, Lagrangian residual circulation patterns, distributions of relative differences induced in the latter by including or not the investigated effects, and convection-dispersion of a passive solute.

#### 1. Introduction

Environmental modelling of a tidal basin generally requires long-term hydrodynamic and transport simulations. For such a task, either *intratidal* and *intertidal* mathematical models could be seen as proper tools from a cost-benefit point of view, depending on the actual time extent of the simulations required for the specific problem to be solved (weeks, months, years, etc.). However, whatever the model used, one is essentially interested in the net (residual, *intertidal*) transport over a time extent of the order of the period of a representative tidal component - typically, 12-24 hours - rather than in a detailed description of the motions occurring at a smaller (*intratidal*) time scale.

It is well known that residual transport is strongly influenced by the nonlinearities acting in water motion (Van de Kreeke, 1976; Zimmermann, 1979)

---

<sup>1</sup>Research carried out with the financial support of Sardinia Regional Authorities.

<sup>2</sup>Research Engineer, CRS4, Centro di Ricerca, Sviluppo e Studi Superiori in Sardegna - Centre for Advanced Studies, Research and Development in Sardinia, Via Nazario Sauro 10, 09123 Cagliari, Italy, E-mail: balzano@crs4.it.

and usually at least one order of magnitude smaller than the tidal excursion. Thus, typical schematizations that are commonly accepted - and acceptable, indeed - when dealing with turbulence-time-averaged quantities could no longer be so when, based on the relevant, intratidal, velocity fields, computations of residual fields are to be performed. This, as long as results may be seriously influenced by effects - either physical or numerical - that are minor factors at smaller time scales.

Many studies about residual circulation can be mentioned, concerning fields of quite different characteristics: harbours (Falconer, 1985), estuaries (Cheng and Casulli, 1982), open sea (Maier-Reimer, 1977). A great deal of research work has been done on Mediterranean lagoons, even with environmental safeguard purposes (O' Kane et al., 1990; Avanzi e Fiorillo, 1983; Cioffi e Gallerano, 1990; Dejak et al., 1990; Cioffi et al., 1994; Defina e D'Alpaos, 1994). Indeed, such water bodies are particularly liable to environmental hazards due to their relatively weak refreshment capability. However, fewer studies of their long term dynamics by field-verified mathematical models exist.

As a preliminary step to the implementation of a water quality forecasting system for eutrophic water bodies in the island of Sardinia, the influence of some of the above mentioned effects on residual transport has been analysed by means of intratidal mathematical models. Since the system is to be applied primarily to relatively small and shallow lagoons, the analysis has been carried out on schematic tidal basins whose geo-morphological characteristics resemble those of such natural water bodies. However, several mediterranean tidal basins match these general features as well. The present investigation is then to be seen as a specific contribution, strictly significant for the particular class of water bodies mentioned above.

Moreover, at this stage particular environmental conditions are considered like those eventually determining anoxia in the water body. These are essentially high temperature and the absence of wind, the latter being of major importance for the setup of residual circulations. Results are then to be intended as realistic for time extents not longer than, say, one month, in the summer season.

## 2. Description of numerical experiments

In the numerical experiments the three prototypes shown in fig. (1) have been considered, namely: (a) a completely flat, 1 m deep, basin with a 400 m long by 800 m wide inlet, whose axis coincides with the symmetry axis of the basin, sided by two expansions whose dimensions are 4000 x 4000 m; (b) a similar basin, in which the central, 800 m wide, strip is occupied by a 5 m deep channel; (c) a basin in which the depth varies gradually from 5 m in the central strip to 1 m at the lateral borders of the expansions. The tidal range at the entrance of the inlet is assumed of the order of 1 m; a latitude of 45° is considered. For the three prototypes and for the various effects investigated, comparisons have been made between either the two-dimensional, depth averaged, Lagrangian residual circulation fields and the results of a stochastic convection-dispersion model based on the random-walk technique.

The influence of the following factors on residual transport has been investigated: i) the Coriolis acceleration; ii) the specification of the tidal forcing at the basin inlet; iii) the diffusion coefficient,  $K$ , in the equation of motion; iv) the time weight,  $\alpha$ , of the finite difference implicit scheme for both the divergence of fluxes in the equation of continuity and the gradient of the free surface elevation in the equation of motion.

For the computations of the intratidal velocity fields a 2D finite difference, Eulerian-Lagrangian, hydrodynamic model was employed. This is based on the usual shallow water equations

$$\frac{\partial \eta}{\partial t} + \frac{\partial U}{\partial x} + \frac{\partial V}{\partial y} = 0$$

$$\frac{\partial U}{\partial t} + \frac{\partial(uU)}{\partial x} + \frac{\partial(vU)}{\partial y} + gh \frac{\partial \eta}{\partial x} - K \nabla^2 U - \frac{\tau_{sx}}{\rho} + g \frac{\sqrt{U^2 + V^2}}{k_s^2 h^{7/3}} U - fV = 0 \quad (1)$$

$$\frac{\partial V}{\partial t} + \frac{\partial(uV)}{\partial x} + \frac{\partial(vV)}{\partial y} + gh \frac{\partial \eta}{\partial y} - K \nabla^2 V - \frac{\tau_{sy}}{\rho} + g \frac{\sqrt{U^2 + V^2}}{k_s^2 h^{7/3}} V + fU = 0$$

where  $x, y$  are the cartesian coordinates in the horizontal plane;  $t$ , the elapsing time;  $u, v$  and  $U, V$ , respectively the mean velocity and unit width discharge components in the  $x$  and  $y$  directions;  $g$ , gravity acceleration;  $\eta$ , free surface elevation above a datum;  $h$ , total depth;  $K$ , the horizontal diffusion coefficient;  $\tau_{sx}$  and  $\tau_{sy}$ , respectively the  $x$  and  $y$  components of the surface stress;  $\rho$ , the density of water;  $k_s$ , the Strickler roughness coefficient ;  $f = 2\omega \sin \varphi$ , the Coriolis parameter;  $\omega$ , the angular speed of the earth's rotation;  $\varphi$ , latitude.

A fourth order Lagrangian method for the treatment of the convective terms and a real bidimensional solution of propagation ensures the correct representation of the velocity fields even in the presence of a dramatically irregular bathymetry (Benqué et al., 1982; Balzano, 1993). Lagrangian residual velocity fields were computed on the basis of the following definition (Cheng and Casulli, 1982)

$$\mathbf{v}_{lr}(\mathbf{x}_o, t_o) = \frac{1}{T} \int_{t_o}^{t_o+T} \mathbf{v}[y(\mathbf{x}_o, t), t] dt \quad (2)$$

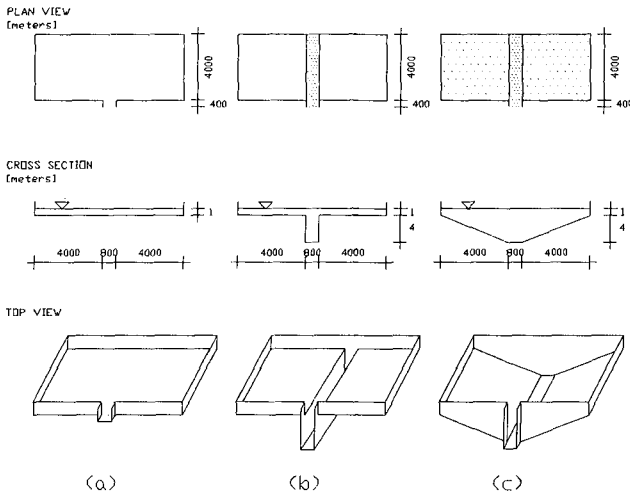


Figure 1: Schematic test basins

where  $\mathbf{v}_{lr} \equiv (u_{lr}, v_{lr})$  is the Lagrangian residual velocity computed in the point of coordinates  $\mathbf{x}_o$  for the tidal phase  $t_o$ ;  $T$  is the tidal period;  $\mathbf{v}(\mathbf{x}, t) \equiv (u, v)$  the eulerian velocity;  $\mathbf{y}(\mathbf{x}_o, t)$  the coordinates of the trajectory of a passive tracer released in the point  $\mathbf{x}_o$  at time  $t_o$ . In the numerical integration (2), the time step was assumed as  $\Delta t = \min \left\{ \frac{\Delta x/n}{u}, \frac{\Delta y/n}{v} \right\}$ , with  $n = 5 \div 10$  and  $\Delta t \leq 10 \div 30$  s. Numerical convergence of the residual velocity fields required time steps down to  $60 \div 120$  s in the hydrodynamic model, corresponding to values of the Courant number  $Cr=0.7 \div 3$ . Incidentally, it is remarked that this suggests the feasibility of resorting to explicit or ADI models for this kind of problems. This, particularly in the case that developments on parallel computers are foreseen to achieve higher computational speed.

In the stochastic transport model a mass of passive solute is represented as a "cloud" of mutually independent particles, subject to the resultant of the deterministic mean flow velocity and random fluctuations (Ghoniem and Sherman, 1985; Maier-Reimer and Sundermann, 1982)). Gaussian random displacements, uncorrelated in the directions normal and tangent to the trajectory were assumed. These are computed on the basis of the relevant longitudinal and transverse components of the dispersion tensor,  $K_l$  and  $K_t$ , as given by Elder formulas, i.e.  $K_l = 5.93 u^*h$ ,  $K_t = 0.23 u^*h$ , where  $u^*$  is the shear velocity. Thus, also dispersion due to vertical shear is represented. Computed values of the above diffusion coefficients are in agreement with those obtained by others with subgrid scale energy techniques for similar water bodies (Pfeiffer et al., 1988).

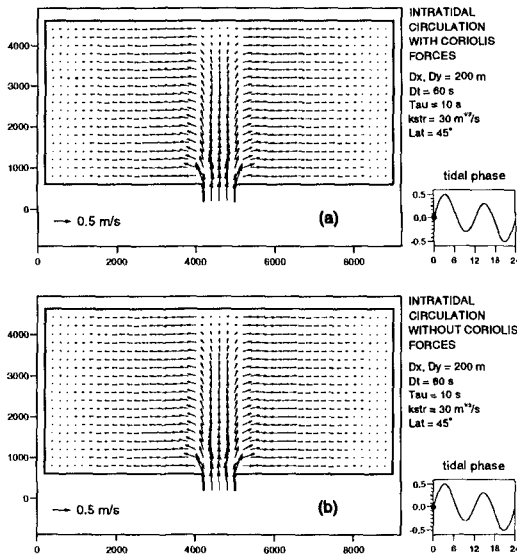


Figure 2: Intratidal circulation velocity field in a flat, 1 m deep, tidal basin with a central, 5 m deep, channel, computed (a) with and (b) without the Coriolis forces

3. Results

3.1 Coriolis acceleration

Classical order of magnitude analysis of the governing equations shows that Coriolis forces are negligible compared to convective terms whenever the Rossby number,  $Ro = \frac{v^*}{2\omega L^*}$ , is large,  $v^*$  and  $L^*$  being a characteristic velocity and length (Pedlosky, 1987). Moreover, they can be small compared to bottom friction in the presence of relatively small water depth and large bottom roughness. As a matter of fact, Coriolis forces are usually regarded as a minor factor in lagoons on the basis of the above arguments (Morandi Cecchi, 1989) and therefore neglected in real case studies (Chignoli e Rabagliati, 1977; Volpi e Sguazzero, 1977; Umgiesser et al., 1988, 1993; Rosso et al., 1993; Cioffi et al., 1994). If only intratidal fields are required, for a number of practical applications it can be agreed upon this choice. As an example, in fig. (2) the instantaneous (i.e. turbulence-time-averaged) velocity fields at mean flood tide in the basin with channel, computed (a) with and (b) without the Coriolis terms included, are shown. For a significant comparison Strickler roughness coefficients down to  $k=30 \text{ m}^{1/3}\text{s}^{-1}$  were assumed in the computations. Indeed, this value corresponds to a rather rough bottom and results from calibrations of models with field data (Umgiesser et al., 1988). In order to avoid problems arising when a uniform level is directly imposed in the presence of the Coriolis forces (Cheng e Walters, 1982), the same symmetrical time series of discharges has been imposed at the inlet as common boundary condition. This was deduced from preliminary computations with the Coriolis terms not included, for a reference mixed tide of 1 m of range. This is composed of a semidiurnal component of amplitude  $a_s = 0.4 \text{ m}$  and a diurnal component  $a_d = 0.141 \text{ m}$  with the same phase.

Clearly, hardly significant differences can be perceived between the two patterns, even in details. Even though differences are more evident near the high and low tide, nonetheless it is agreeable that a reliable description of the instantaneous circulations can be obtained without the inclusion of the Coriolis terms. However, residual velocity fields based on intratidal fields computed including or not the Coriolis terms show significant differences for all the three prototypes, particularly for the flat and the channeled basin. In the former (see fig. (3)), quite different locations of the centers of the macro-vortexes can be observed, while in the latter (see fig. (4)) a large zone of close recirculation is not reproduced without the inclusion of the Coriolis terms. This occurs also in the third basin, but with narrower recirculating eddies. It is to be noted that not only the test basins are given a remarkable roughness, but also they are much smaller than the real water bodies for which Coriolis effect was assumed as negligible in the references previously quoted, i.e. the Venice lagoon ( $550 \text{ km}^2$ ).

A quantitative analysis has been carried out, resulting in curves of the cumulative frequencies,  $F(S)$ , of the relative differences,  $S$ , between the values of the residual velocity components in the grid nodes as computed in the two cases. These are plotted for various tidal phases, to which Lagrangian residual quantities are sensitive (phase 0 = flood, mean tide). Also, these curves are plotted for different threshold values,  $\Theta$ , of the velocity components in order to point out whether large relative differences affect even the greatest velocity components in the residual field. In symbols:

$$S_w(\Theta) = \left| \frac{w_{i,j}^a - w_{i,j}^b}{w_{i,j}^a} \right| \quad \text{with} \quad w_{i,j}^a \geq \Theta \quad \text{OR} \quad w_{i,j}^b \geq \Theta ; \quad w = u_r, v_r$$

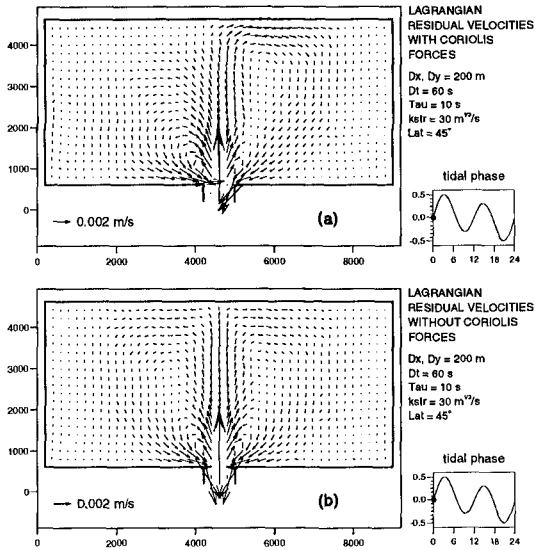


Figure 3: Lagrangian residual circulations in a flat, 1 m deep, tidal basin computed (a) with and (b) without the Coriolis forces

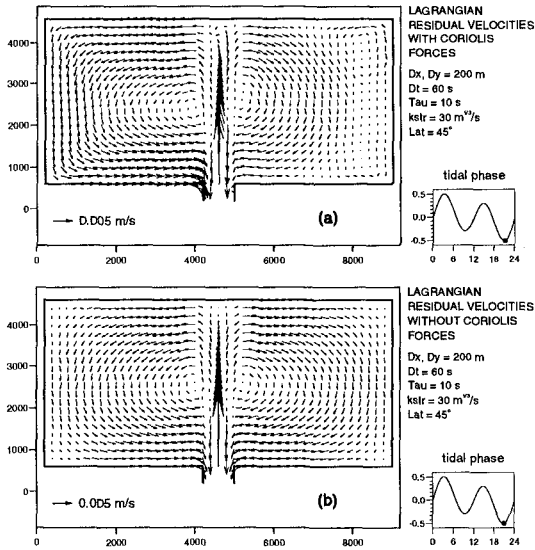


Figure 4: Lagrangian residual circulations in a flat, 1 m deep, tidal basin with a central, 5 m deep, channel, computed (a) with and (b) without the Coriolis forces

In fig. (5a-c) such curves computed for the three basins in the cases that Coriolis forces were included or not are shown. For instance, for the flat basin (fig. (5c)) it is seen that not only the about 1100÷1350 values of residual velocity components greater than 0.0001 m/s – whatever the tidal phase – but also the 26 values greater than 0.002 m/s – for the 0/8 tidal phase – still exhibit significant relative differences, i.e. even greater than 100%. More impressive

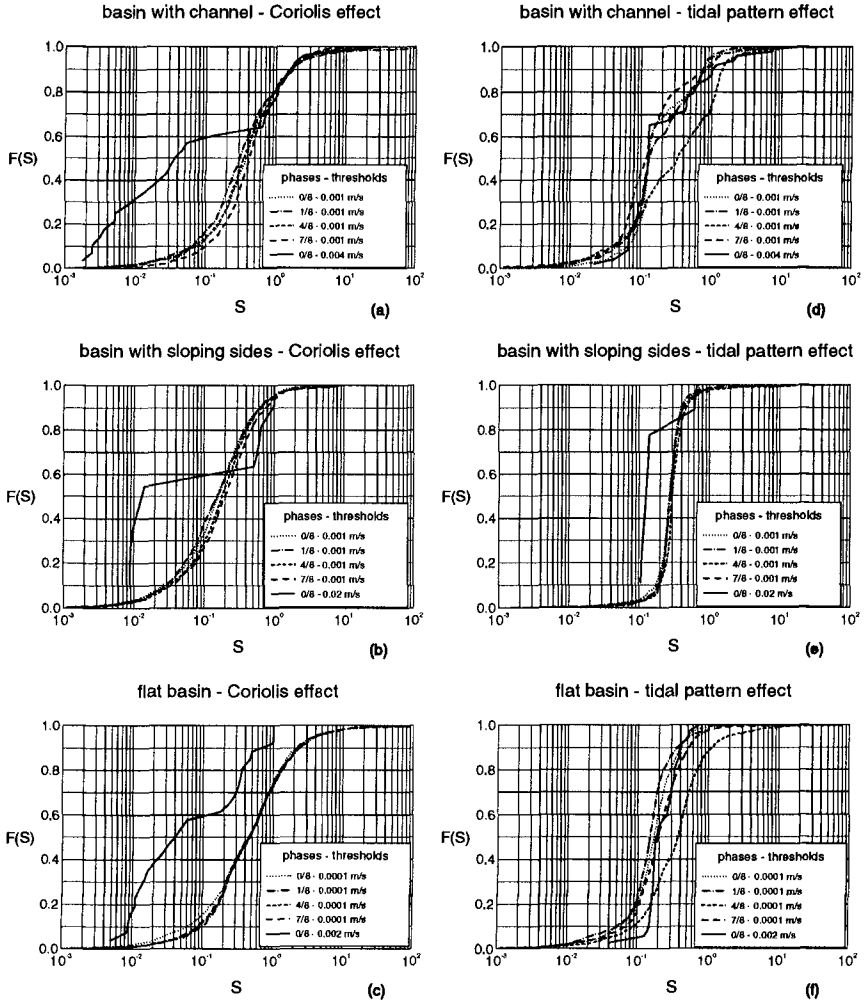


Figure 5: Curves of the cumulative frequencies,  $F(S)$ , of the relative differences,  $S$ , between residual velocities components computed for the three test basins (a-c) with the mixed tide including or not the Coriolis terms and (d-f) with the Coriolis terms considering the semidiurnal or the mixed tide

results obtained with the stochastic transport model will be shown further on, together with analogous results from analysis of the effect of the tidal pattern.

### 3.2 Specification of tidal wave at open boundaries

The second comparison has been carried out between the specification of a semidiurnal and a mixed tide (see fig. (6c,b)) as boundary condition of the hydrodynamic model. Indeed, the latter is the basic pattern of a possibly more complicated real tide like that shown in fig. (6a). This general behaviour can be observed at Mediterranean coasts, as well as at many other sites in the world. However, in literature cases can be mentioned in which, given a real irregular pattern, the semidiurnal one is assumed either, generically, for the sake of simplicity or since it is assumed that very refined results should not be expected when a necessarily rough specification is given as to any other parameter or forcing – typical is the case of wind – included in the model (Cheng and Casulli, 1982). It seems then useful to elucidate what the consequences of this choice might be if a less rough description of residual circulation is desired in the case that no other important external forcing is acting on the field. As mentioned earlier, this is not an unacceptible abstraction since these are exactly the conditions in which, e.g. anoxia phenomena occur in an eutrophic water body. However, the present investigation is, in turn, somewhat simplified in that the tidal amplitude variability in the syzygial period is not taken into account. The present investigation may then be regarded as a first attempt to define a suitable representative tidal pattern to be used in practical applications to approximate the real behaviour in the intertidal approach.

The mixed tide to be approximated is the one already mentioned in section 3.1 and shown in fig. (6b). At first, results obtained with tides of equal amplitude  $a = 0.5$  m (fig. (6c)) have been compared. Then, tentative alternative specifications of the semidiurnal tide have been tried, namely: i) the single semidiurnal component extracted from the mixed tide ( $a = a_s = 0.4$  m); ii) the semidiurnal tide whose mean energy equals that of the mixed tide ( $a = \sqrt{a_s^2 + a_d^2} = 0.424$  m), mean tidal energy over the period,  $T$ , being defined as

$$E = \frac{1}{T} \int_T \eta^2 dt$$

In no case significant improvements were obtained as to the similarity of numerical results. In fig. (5d-f) the curves of cumulated frequencies of relative

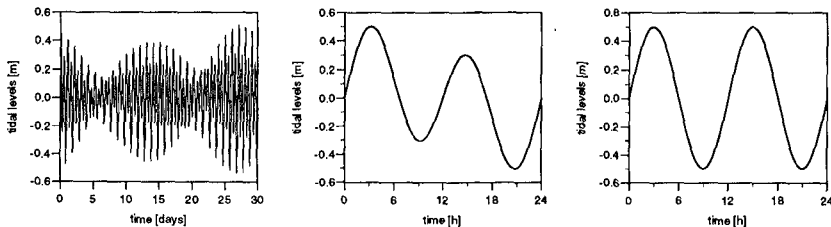


Figure 6: Simplification of tidal patterns: (a) typical real behaviour of a Mediterranean tide, (b) mixed pattern, (c) semidiurnal pattern

differences computed for the three basins for the comparison to the semidiurnal tide of equal range are shown.

### 3.3 Simulations of convection-dispersion

Numerical simulations of convection-dispersion of a passive solute released in various points of the basins confirmed the significance of the previously mentioned differences.

In the flat basin the spreading of the tracers is very weak and regular. Indeed, according to the simple gaussian model of dispersion (Adams and Baptista, 1987), the second central moment of the mass distribution

$$D_{sq}^2 = \frac{1}{N} \sum_{i=1}^N (x_i - x_c)^2 + (y_i - y_c)^2$$

where  $x_i$ ,  $y_i$  are the coordinates of the  $i$ -th particle of the ensemble of  $N$  particles, and  $x_c$ ,  $y_c$  are the coordinates of the center of mass, was found to be fairly linearly proportional to the elapsed time for a specified tidal phase, at least after a sufficiently long time from the release. This is shown in fig. (7) for the release point No. 1 of fig. (8), in the presence of both mixed tide and Coriolis forces. Although the alternate stretching and contracting behaviour of the cloud is governed essentially by the mean velocity gradients, the order of magnitude of the ratio  $D_{sq}^2/2t$  is as that of the intratidal diffusion coefficients considered in the simulation of random fluctuations.

Under the above conditions of regularity of diffusion, exclusive reference can be made to the position of the center of mass for the comparison of the effects of the tidal pattern and the Coriolis forces. Results are shown in fig. (8) for three points of release of the mass of solute and for the four possible combinations of the above factors. Trajectories followed by the centers of mass over a time extent of 20 days are plotted with a time step equal to the period of the relevant tidal pattern, so that tidal excursion is not resolved. It is apparent that

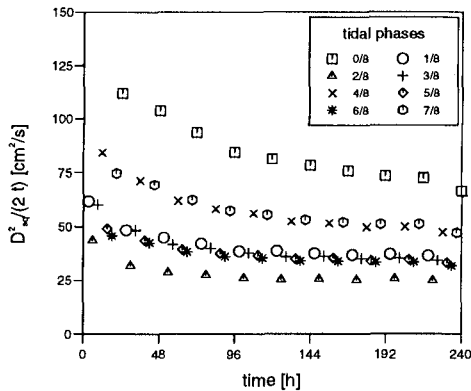


Figure 7: Ratios  $D_{sq}^2/(2t)$  computed at fixed tidal phases for a cloud of passive solute transported in the flat basin under the effect of both the mixed tide and the Coriolis forces - release point No. 1 of fig. (8)

neglecting of the Coriolis forces leads to a much more unrealistic simulation of the transport phenomenon compared to the approximation of the mixed tide by the semidiurnal one.

In the channeled basin, depending on the location of the release point, intratidal dispersion can be completely dominated by the spread induced by noticeable mean velocity gradients. Indeed, in that zones intratidal dispersion is only responsible for the initial, near field, displacement from which the second factor leads to a spread of a greater order of magnitude. In fig. (9a-f) the displacements of clouds of solute after four days from the release in two points of the basin are shown. Depending on the location of the point of release, a different relative importance of the Coriolis forces and the tidal pattern in the convection-dispersion process can be perceived. In particular, near the shore, just like in the flat basin, considering the Coriolis forces is much more important than exactly specifying the tidal pattern. However, in the proximity of the channel both factors must be properly represented for a correct reproduction of the dispersion process.

It is apparent that the reason of this behaviour is to be found in the major role played by the channel in the whole dynamics of the water body, it being able to produce a circulation that is one order of magnitude stronger than in the flat basin. Apparently, the Coriolis forces act more as a direct driving factor of the circulation in the flat areas of both basins. Instead, in the areas influenced by the channel their role is mainly that of inducing different interactions between the expansions and the channel itself, whose presence, along with the associated strong velocity gradients, is indeed responsible of the important convection and dispersion at the intertidal scale. If boundary conditions like the tidal wave are changed, then the low hydraulic conductivity of the flat areas - in particular, of the inlet - causes the effects of the changes to be damped as well. Instead, the major conductivity of the channel causes the features of an important driving mechanism, and so the resulting features of circulation, to be remarkably modified too.

The basin with sloping sides behaves essentially like the channeled one, as far as analogous conditions at the inlet are involved. This is shown in fig. (10a-f) for the same points and initial tidal phases of release as for the channeled basin. In particular, for the release in the proximity of the channel, while considering the mixed pattern makes only a small part of the particles to be out of the domain after four days, none of them remains within it if the semidiurnal tide is considered, regardless of the inclusion of the Coriolis terms.

### 3.4 Diffusion coefficient and numerical time weight

Let us consider the following simplified form of the x-momentum equation drawn from system (1):

$$\frac{\partial U}{\partial t} + gh \frac{\partial \eta}{\partial x} + \gamma U = 0 \quad (3)$$

where  $\gamma U$  is the linearised bottom friction term. This can be discretised on a fully staggered, Arakawa-C grid as

$$\frac{U_{i+1/2,j}^{n+1} - U_{i+1/2,j}^n}{\Delta t} + \alpha \left( gh_{i+1/2,j}^{n+1} \frac{\eta_{i+1,j}^{n+1} - \eta_{i,j}^{n+1}}{\Delta x} \right) \quad (4)$$

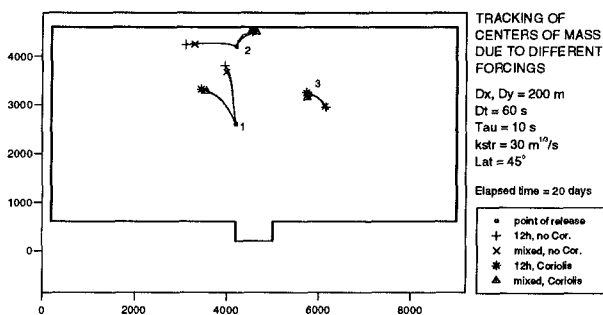


Figure 8: Pathlines of the centers of mass of clouds of a passive solute dispersing in a flat, 1 m deep, tidal basin under different forcing conditions

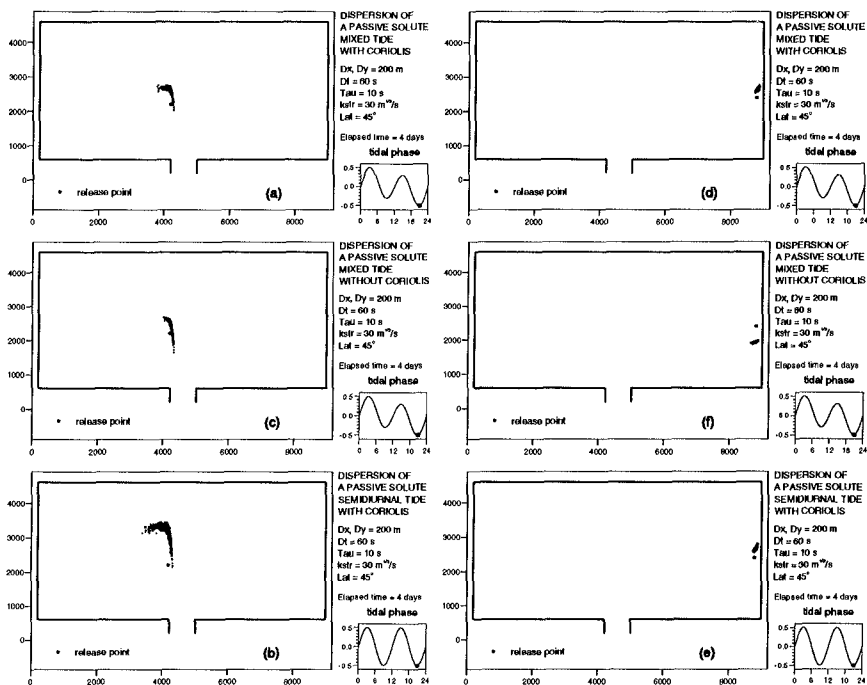


Figure 9: Advection-dispersion of a passive solute in a flat, 1 m deep, tidal basin with a central, 5 m deep channel, four days after release in two points, computed for a mixed tide (a,d) with and (b,e) without the Coriolis forces, and (c,f) for a semidiurnal tide of equal range with the Coriolis forces

$$+ (1 - \alpha) \left( g \bar{h}_{i+1/2,j}^n \frac{\eta_{i+1,j}^n - \eta_{i,j}^n}{\Delta x} \right) + \gamma U_{i+1/2,j}^{n+1} = 0$$

where  $\alpha = 0.5 \div 1$  is required for a stable discretization. Analysis of the relevant truncation error shows that using scheme (4) in numerical computations equals solving

$$\frac{\partial U}{\partial t} + gh \frac{\partial \eta}{\partial x} + \gamma U = - \left[ \left( \frac{1}{2} - \alpha \right) \frac{\partial^2 U}{\partial t^2} + (1 - \alpha) \gamma \frac{\partial U}{\partial t} \right] \Delta t + O(\Delta t^2, \Delta x^2, \Delta y^2)$$

regardless of the method used for the linearisation of the barotropic pressure gradient. This holds also for a fully non-conservative analog of equation (3), involving velocity components alone. In the absence of bottom friction, the scheme can be made of second order in time by letting  $\alpha = 0.5$ , while values greater than 0.5 provide a damping effect (Casulli and Cattani, 1993). Since this effect, even though not remarkable, is nonetheless clearly perceivable at the intratidal time scale, a check on its importance at the intertidal scale has been done.

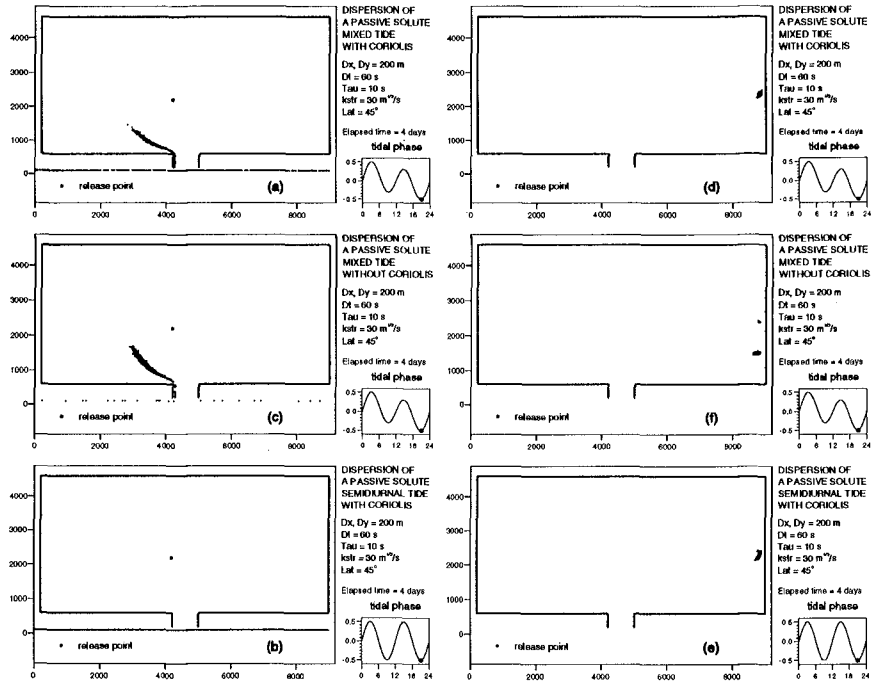


Figure 10: Advection-dispersion of a passive solute in a tidal basin with a central, 5 m deep, strip and sloping sides, four days after release in two points, computed for a mixed tide (a,d) with and (b,e) without the Coriolis forces, and (c,f) for a semidiurnal tide of equal range with the Coriolis forces

The effect of diffusion terms in equations (1) is also often considered negligible in current simulations in lagoons, provided that sufficiently small space and time scales are considered in the computations (Pfeiffer et al., 1988; Rosso et al., 1993; Umgiesser et al., 1993).

As far as regards the parameter,  $\alpha$ , and the diffusion coefficient,  $K$ , comparisons have been carried out, for the channeled basin only, between results obtained in a reference case (the above mixed tide of 1 m of range,  $K=0$ ,  $\alpha=0.5$ , i.e. Crank-Nicholson scheme), and two cases differing respectively by  $K=1 \text{ m}^2/\text{s}$  and  $\alpha=1$  (fully implicit scheme). These values represent a strictly upper limit value for the latter parameter and a reasonable one, though roughly estimated, for the former, depending on the characteristics of both the basin and the motion. In fig. (11a,b) the relevant curves of relative differences are shown. Though the channeled basin was expected to be, among the three, the most sensitive to changes in the above mentioned parameters, results are apparently much less significant compared to the cases of Coriolis forces and tide specification.

4. Conclusions

Some features of long term transport in shallow and relatively small lagoons under a relatively weak tidal forcing alone have been analysed. Results are then applicable to Mediterranean tidal basins in the absence of wind, i.e. in conditions like those eventually leading to anoxia in the water body.

It has been shown that the usual assumption of neglecting Coriolis forces in this kind of basins is acceptable only for the purpose of determining the general characteristics of intratidal circulation. Indeed, this factor proved essential to the correct simulation of long term transport in all the three prototypes considered. Potentially dangerous mistakes of practical interest in applications have been shown. A mixed tidal pattern proved well approximated by a semidiurnal one of equal range in a flat basin in which the tidal range is substantially damped at the inlet, as well as in the peripheral, shallower areas of basins in which propagation of the tidal wave is allowed to a larger extent. In the latter, a more realistic tidal pattern is required for a correct simulation of convection-dispersion in areas

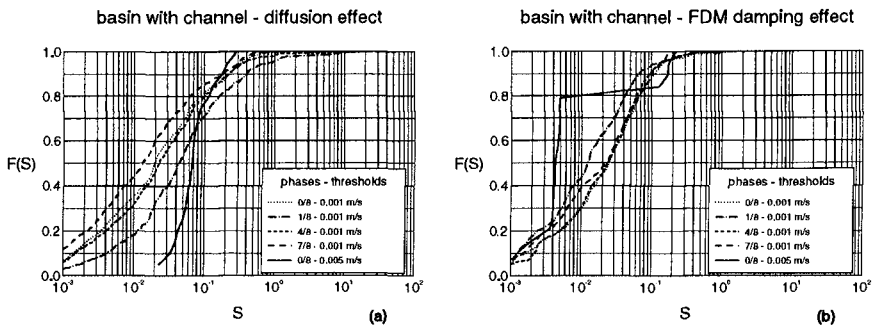


Figure 11: Curves of the cumulative frequencies,  $F(S)$ , of the relative differences,  $S$ , between residual velocities components computed for the basin with channel with the mixed tide and Coriolis forces (a) including or not the diffusion terms with  $K = 1 \text{ m}^2/\text{s}$  and (b) selecting  $\alpha = 0.5$  and  $\alpha = 1$  in the numerical discretization (4) of the propagation terms

characterized by relatively strong velocity gradients in the hydrodynamic field.

Though numerical results should always be regarded with caution even when an accurate check is done on numerical convergence and a robust and accurate model is employed, particularly in the presence of a highly irregular bathymetry (D'Alpaos et al., 1992), nonetheless it seems that, if not exactly the numerical entity of the mentioned differences, at least the remarkable differences shown as to the circulation patterns should be regarded as really meaningful.

On the basis of the above results, it seems that a representation of the long term transport due to a real tide of variable amplitude in the syzygial cycle in terms of residual fields for semidiurnal tides of correspondingly varying amplitudes can be tried for basins like the flat one considered in this study.

On the other hand, residual circulation seems to be less sensitive even to reasonably high values of the diffusion coefficient, which, however, could not be assigned an accurate value at the start of the art. Even less significant is the effect of the numerical time weight  $\alpha$ , of a standard implicit discretization scheme for spatial derivatives, whose smoothing effect when equal one is not so much important on tidal waves compared to short and high-frequency ones.

#### Appendix. - References

- Adams, E.E., and Baptista, A.M., (1987). Ocean Dispersion Modelling. In *Enciclopedia of Fluid Mechanics, Gulf Publishing Company, v. 6*, 865-895.
- Avanzi, C., and Fiorillo, G., (1983). Modello di dispersione bidimensionale intermareale della laguna di Venezia. Pub. 352 Ist. di Idraulica Univ. di Padova.
- Balzano, A., (1993). Sulla modellazione matematica di onde lunghe mediante metodi euleriano-lagrangiani bidimensionali. *PhD Thesis*, Milano.
- Benqué, J.P., Cunge, J.A., Feuillet, J., Hauguel, A. and Holly, F.M. Jr, (1982). New Method for Tidal Current Computation. *Journal of Waterways, Port, Coastal and Ocean Division, A.S.C.E., v. 108*, 396-417.
- Casulli, V., and Cattani, E., (1993). Stability, Accuracy and Efficiency of a Semi-Implicit Method for Three-Dimensional Shallow Water Flow. *Computer and Mathematics with Applications*.
- Cheng, R.T. and Casulli, V., (1982). On Lagrangian Residual Currents With Application in South San Francisco Bay. *Water Res. Research, 18, 6*, 1652-1662.
- Cheng, R.T. and Walters, R.A., (1982). Modelling of Estuarine Hydrodynamics and Field Data Requirements. In: *Finite Elements in Fluids, Ed. Gallagher et al. 4, John Wiley, New York*, 89-108.
- Chignoli, C., and Rabagliati, R., (1977). A Two-Dimensional Model for the Lagoon of Venice: Acqua Alta and Modular Sluices. *Proc. XVII IAHR Congress, v. 3, Baden Baden, FRG*, 393-399.
- Cioffi, F., and Gallerano, F., (1990). Effetti dei ricambi idrici forzati sul contenimento delle crisi anossiche nella laguna di Orbetello *Atti del XXII Convegno di Idraulica e Costruzioni Idrauliche, Cosenza*, 149-162
- Cioffi, F., Di Eugenio, A., and Gallerano, F., (1994). Simulation model for forecasting anoxic crisis in lagoons. *Proc. of Conference on Computer Techniques in Environmental Studies, San Francisco*, 107-120
- D'Alpaos, L., Defina, A. and Zovatto, L., (1992). Correnti residue fisiche e numeriche in un bacino a marea indagata con schemi di calcolo bidimensionali. *Atti del 29° Convegno di Idraulica e Costruzioni Idrauliche, D.139, Firenze*.

- Defina, A., and D'Alpaos, L., (1994). Una breve nota sui coefficienti di dispersione intermareale. *Atti del XXIV Convegno di Idraulica e Costruzioni Idrauliche, Napoli, Italy*, T1 49-56
- Dejak, C., Franco, D., Pastres, R., and Pecenic, G., (1990). A 3-D Eutrophication-diffusion Model of the Venice Lagoon: Some Applications. In: *Coastal and Estuarine Studies, Vol. 38, R.T. Cheng Ed., Residual Currents and Long-term Transport, Springer Verlag New York.*, 526-538.
- Falconer, R.A., (1985). Residual Currents in Port Talbot Harbour: A Mathematical Model Study. *Proc. Inst. Civ. Engrs., London, Part 2, 79, Mar.*.
- Ghoniem, A.F., and Sherman, F.S., (1985). Grid Free Simulation of Diffusion Using Random Walk Methods. *Journal of Computational Physics, 61*, 1-37
- Maier-Reimer, E., (1977). Residual Circulation in the North Sea Due to the M2-Tide and Mean Annual Wind Stress. *Deutsche Hydrographische. Zeitschrift, 30*, 69-80.
- Maier-Reimer, E., and Sundermann, J., (1982). On Tracer Methods in Computational Hydrodynamics. In: *Engineering Applications of Computational Hydraulics, Eds. Abbott, M.B. and Cunge, J.A., vol. 1, Pitman Publ. Inc.*, 198-219.
- Morandi Cecchi, M., (1989). Study of the behaviour of Oscillatory Waves in a Lagoon. *Int. Journal of Numerical Methods for Engineers, v.27*, 103-112.
- O'Kane, J.P., Suppo, M., Todini, E., Turner, J., (1990). Project for Optimal Management of the Goro Lagoon by Means of a Three-Dimensional Hydrodynamical-Diffusive Model. In: *Computational Methods in Surface Hydrology, Brebbia, C.A. et al. Eds., Venice, Italy*, 139-147.
- Pedlosky, J., (1987). Geophysical Fluid Dynamics. *Springer Verlag New York.*
- Pfeiffer, K.D., Duwe, K.C., and Sundermann, J., (1988). A High-Resolving Eulerian Current and Lagrangian Transport Model of the Lagoon Valle Vallona. In: *Computer Modelling in Ocean Engineering, Schrefler, B.A. and Zienkiewicz, O.C. Eds., Balkema, Rotterdam Brookfield, Netherland*, 393-400.
- Rosso, M., Fettweis, M., and Yu, C.S., (1991). Tidal Flow Simulation in the Lagoon of Venice. *Proc. II International Conference on Computer Methods and Water Resources, Marrakesh, Morocco.*
- Umgiesser, G., Sundermann, J. and Runca, B., (1988). A Semi-Implicit Finite Element Model for the Lagoon of Venice. In: *Computer Modelling in Ocean Engineering, Schrefler, B.A. and Zienkiewicz, O.C. Eds., Balkema, Rotterdam, Netherland*, 71-79.
- Umgiesser, G. and Bergamasco, A., (1993). A Staggered Finite Element Model of the Venice Lagoon. In: *Proc. VIII International Conference on "Finite Elements in Fluids", Barcelona, Spain.*
- Van de Kreeke, J., (1976). Tide-Induced Mass Transport; a Flushing Mechanism for Shallow Lagoons. *Journal of Hydr. Res., v. 14, n° 1.*
- Volpi, G., Sguazzerio, P., (1977). La propagazione della marea nella laguna di Venezia: un modello di simulazione ed il suo impiego nella regolazione delle bocche di porto. *Rivista Italiana di Geofisica, v. IV (1,2).*
- Zimmermann, J.T.F., (1979). On the Euler-Lagrange Transformation and the Stokes' Drift in the Presence of Oscillatory and Residual Currents. *Deep Sea Research, 26 A*, 505-520.